International Journal of Multimedia and Ubiquitous Engineering
Vol.11, No.3 (2016), pp.67-80
http://dx.doi.org/10.14257/ijmue.2016.11.3.07

Application of Modified Empirical Mode Decomposition Method to Fault Diagnosis of Offshore Wind Turbines

Ming-ShouAn and Dae-Seong Kang[1]

Dong-A University, Dept. of Electronics Engineering, 37 Nakdong-daero 550 beon-gilSaha-gu, Busan, Korea
dskang@dau.ac.kr

Abstract

In recent years, many countries have actively studied wind power generation as a means of realizing low-carbon green growth through a new renewable energy source. The most efficient method of securing the stable operation of wind turbines and reduce maintenance costs is monitoring and analyzing their operational status in realtime through a remote monitoring system. Remote monitoring systems employ various sensor technologies and the Wireless Sensor Network to collect and transmit data on the status of individual parts in realtime, and they diagnose faults through a signal analysis system. Application of the fault analysis method can reduce fault resolution times and minimize losses. In this study, signals collected from wind turbines were analyzed, and their characteristics were extracted through empirical mode decomposition (EMD). In the experiment, EMD learning was carried out using the following fault signals as examples: The back-propagation (BP) neural network algorithm with generator vibration, an unbalanced rotor, and a bearing misalignment fault. This article proposes a method of diagnosing faults through signal analysis and recognition, and it demonstrates the validity of the method through a simulation.

Keywords*: Wind power generation, remote monitoring system, various sensor technologies, Wireless Sensor Network, empirical mode decomposition, neural network algorithm*

1. Introduction

Due to the exhaustion of fossil fuels, soaring oil prices, and the elevating prices of raw materials, securing new renewable energy sources is a crucial task upon which the survival of global society depends. Many countries have begun to encourage not only the research and development of renewable energy, but also the commercialization of related industrial technologies. “New renewable energy” refers to energy resources that can be converted to eco-friendly and renewable energy forms, including solar light, solar heat, bio-energy, wind power, hydropower, ocean energy, and geothermal power [1].

Large-scale wind power generation complexes have already been established. The scale-up of wind turbines has enabled wind power to extend to the sea, which offers large spaces and abundant wind resources. However, the cost of maintaining offshore wind power accounts for 23–35% of overall energy production costs, given that wind turbine towers are high, scaled-up blades are large, and offshore complexes are difficult to approach compared with those on land. Thus, large-scale and offshore wind turbines necessitate the development of technologies to secure operational reliability by means of the real-time monitoring of faults in individual turbine parts [2].

The most efficient method of securing stable operation and reduce maintenance costs is monitoring and analyzing wind turbines’ operational status in realtime

ISSN: 1975-0080 IJMUE

through a remote monitoring system [3-4]. Remote monitoring systems employ various sensors to collect and transmit data on the status of individual parts in realtime and diagnose faults through a signal analysis system. Taking measures accordingly can reduce fault resolution times and minimize losses.

A wind power generator consists of a wind turbine that converts wind energy into mechanical energy and a generator that converts mechanical energy into electric energy. A wind turbine is operated intermittently according to changes in wind speed. Due to wind speed fluctuation and various environmental factors, mechanical fault signals are complex, time-varying, and unstable, making faults in wind turbines difficult to identify. The system used to monitor wind turbine condition analyzes data collected from vibration sensors installed in turbines' major components, including the generator, gearbox, main bearing, shaft, and yaw system. For wind turbines that are offshore, however, the NI WSN (Wireless Sensor Network) environment is established to address limitations in accessing the sea; the vibration signals of the individual parts can be collected, transmitted, and analyzed remotely through the wireless network. Signal data collected in this way are used to determine whether there is a fault through the application of a signal analysis method in the remote monitoring system [5]. Typical signal analysis methods include the Fourier transform method, in which time domain signals are converted to the frequency domain for analysis, and the wavelet transform method, in which time-varying frequency elements can be identified by expressing signal characteristics in the frequency-time domain. A fast Fourier transform algorithm was used to detect rotor faults in the induction machine in one study [6], while another study used a sort of Fourier transform method to detect gearbox and coil faults [7]. In this study, the suggested method involves analyzing the spectrum characteristics of fault signals using the Hilbert–Huang transform (HHT) based on empirical mode decomposition (EMD). We propose an analytical method of fault diagnosis by automatically monitoring the status of wind turbines using the spectrum characteristics of the individual segments extracted by HHT as the input values for the neural network.

2. Paper Method of Analyzing Fault Signals of Wind Turbines

2.1. Hilbert–Huang Transform

In this method, time-frequency signals are decomposed into signals with different internal frequency elements by EMD [8-10]. With respect to the individual decomposed signals, the Hilbert–Huang transform is performed to acquire instantaneous frequency signals. The Hilbert–Huang transform was first introduced in 1998 by Norden E. Huang. The signals decomposed by EMD are called intrinsic mode functions (IMFs), because the individual signals have different frequency elements. In this article, the frequency signals collected from the generator were decomposed into IMFs by EMD. This article also suggests a method for diagnosing generator faults using the characteristics of the decomposed IMFs.

The elements decomposed into the IMF refer to the status, where the magnitudes of the maximum and minimum values are locally symmetrical with respect to 0 in the physically instantaneous frequency range. The IMF elements can be expressed as the sum of c1(t), c2(t),…, cn(t) and the remainder, rn(t), until the time indicated in the following equation.

$$x(t) = \sum_{j=1}^{n} c_j(t) + r_n(t) \quad (2.1)$$

The equation indicates that the data can be decomposed into individual IMFs and remainders, and the original data can be composed with the decomposed values. The IMFs should satisfy the following two conditions:

(1) The number of extreme in the data and the number of zero crossings are the same or differ by 1.

(2) The mean of the top and bottom envelopes is 0 at all points.

Table 1.The Algorithm of EMD

EMD Algorithm
EMD is the empirical method for obtaining an IMF. An IMF is obtained through the following steps. (1) The given data $x(t)$,which input vibration signals from the wind turbine,are set as $s_k(t)$ as in the following equation, and 1 is substituted for k:$s_1(t) = x(t)$. (2) With all local maximum values of$s_k(t)$, the top envelope is obtained using the cubic spline. (3) As in Step (2), the bottom envelope is obtained with the local minimum values. At this point, all data should be present between the top and bottom envelopes. (4) The instantaneous mean of the top and bottom envelope, $m_k(t)$, is calculated, and $h_{n,k}(t)$ is calculated as the difference between $s_k(t)$ and $m_k(t)$). In$h_{n,k}(t)$, n denotes the nth IMF, and $k$denotes the number of times that the repeated calculation is performed to calculate the IMF. Thus, $h_{n,k}(t) = s_k(t) - m_k(t)$. (5) If $h_{n,k}(t)$ does not meet the two conditions of the IMF, k is increased by 1. Steps (2), (3), and (4) are repeated with $h_{n,k}(t)$ as $s_k(t)$ until the two conditions of the IMF are satisfied. If $h_{n,k}(t)$ meets the two conditions of the IMF,$h_{n,k}(t)$ becomes the nth IMF of $c(t)$, which is $c(t)$. Thus, $c(t) = h_{n,k}(t)$. (6) Let$r_n(t)$ be the remainder of $s_k(t)$, from which$c_n(t)$, the kth IMF element, is subtracted, $r_n(t) = s_k(t) - c_n(t)$. (7) The remainder $r_n(t)$ is set as $s_k(t)$. To obtain the $(n+1)$th IMF, which is $c_{n+1}(t)$, *n* is increased by 1, and Steps (2), (3), (4), (5), and (6) are repeated. If $r_n(t)$ cannot satisfy the IMF conditions any longer, or if there is almost no vibrant element in the signal, the repeated process is stopped.

2.1. Transform Improvement Suggestion for Enveloping

If we obtain an exact EMD division result, it needs accurate envelope calculation. The general EMD analysis method uses cubic spline interpolation to obtain the envelope. This method requires knowledge of all sample points from $\mathrm{P_1}$to $\mathrm{P_n}$, and then uses two points in the curve to predict a new curve. However, this method causes overshoot when each approximate sample point has a lengthened interval and the gap of curvature is big. Therefore, following thesis 12, the causes of overshoot of Cubic Spline Interpolation, we focus on keeping each point's interval constant and on preventing the overshoot interval of approximate sample points from changing much. This is done to obtain a curve between two points that use five sample points from $\mathrm{P_{i+2}}$ to$\mathrm{P_{i-2}}$. This point differs from Cubic Spline Interpolation; Cubic Spline Interpolation uses two points that are approximate, and this method uses five sample points. However, according to the change in the interval of points, obtaining the curve length is also different. Obtaining signals from the generator occurs irregularly, and frequency changes appear frequently [9–10]. Therefore, this problem also regards the points problem, which involves big changes. It is theory of the way in which the interval between two points is modulated, and then we can

estimate the curve more exactly. It could reduce the overshoot phenomenon. In order to obtain a curve $C_i(t)$ between two points, we can obtain imaginary sample points. This has to satisfy a condition.

Table 2. The First Stage of Improvement Overshooting with Cubic Spline Interpolation

(1) If $2L_i < L_{i-1}$,

The distance between points P_i and P_{i+1} is shorter than 1/2 of the distance between points P_{i-1} and P_i,

$$[P_{i-2}, P_{i-1}, P_i, P_{i+1}, P_{i+2}] \Rightarrow [P_{i-1}, C_{i-1}(0.5), P_i, P_{i+1}, P_{i+2}]$$

$C_{i-1}(0.5)$ was used instead of P_{i-1}.

$C_{i-1}(0.5)$ appears as a time-based centered coordinate, which was drawn previously as $C_i(t)$.

It used the centered coordinate between P_{i-1} and P_i.

Thus, it uses $C_{i-1}(0.5)$ instead of P_{i-1}, and P_{i-2}, P_{i-1}. $C_{i-1}(0.5)$ is obtained using the $C_i(t)$ formula.

$$C_i(t) = P_i(2t^3 - 3t^2 + 1) + P_{i+1}(-2t^3 + 3t^3) + P_i'(t^3 - 2t^2 + t) + P_{i+1}'(t^3 - t^2)$$

where it is assumed that $0 \le i \le n-1$, $0 \le t \le 1$, $C_i(0) = P_i$, $C_i(1) = P_{i+1}$

$$C_i(0.5) = \frac{P_i + P_{i+1}}{2}$$

In this method, the interval between points P_{i-1} and P_i is relatively big. Therefore, using $C_{i-1}(0.5)$ reduces the interval of the sample points.

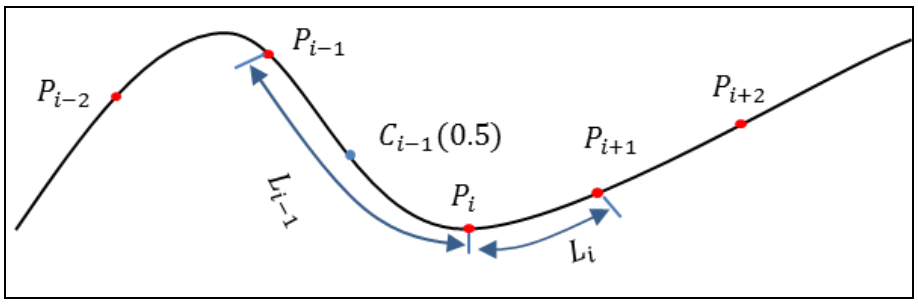

Figure 1. Cubic Spline Interpolation with 5 Points (Case 1)

Table 2. The Second Stage of Improvement Overshooting with Cubic Spline Interpolation

(2) If $2L_i < L_{i+1}$,
The distance between P_i and P_{i+1} is smaller than 1/2 of the distance between P_{i-1} and P_i, $[P_{i-2}, P_{i-1}, P_i, P_{i+1}, P_{i+2}] \Rightarrow [P_{i-2}, P_{i-1}, P_i, P_{i+1}, \frac{P_{i+1}+P_{i+2}}{2}]$ In this case, the interval of points between P_{i+1} and P_{i+2} is relatively big. Therefore, using $\frac{P_{i+1}+P_{i+2}}{2}$ instead of P_{i+2} can reduce the sample points interval. In other words, $\frac{P_{i+1}+P_{i+2}}{2}$ is $C_{i+1}(0.5)$.

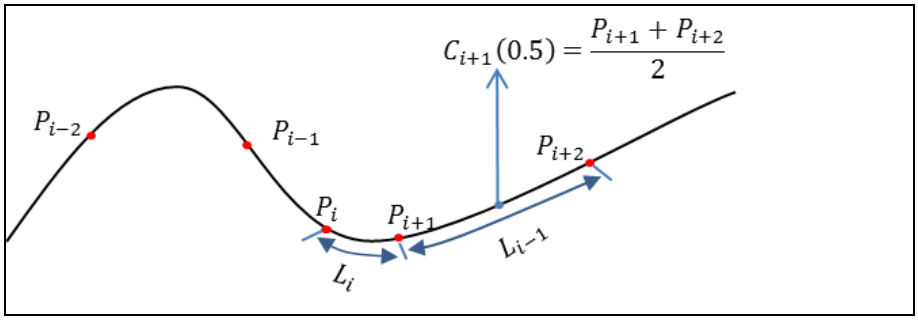

Figure 2. Cubic Spline Interpolation with 5 Points (Case 2)

Table 2. The Third Stage of Improvement Overshooting with Cubic Spline Interpolation

(3) if $2L_i < L_{i-1}$ and $2L_i < L_{i+1}$
$[P_{i-2}, P_{i-1}, P_i, P_{i+1}, P_{i+2}] \Rightarrow [P_{i-1}, C_{i-1}(0.5), P_i, P_{i+1}, \frac{P_{i+1}+P_{i+2}}{2}]$

If step (1) and step (2) occur at the same time, all techniques using step (1) and step (2) are used to reduce the interval of sample points.

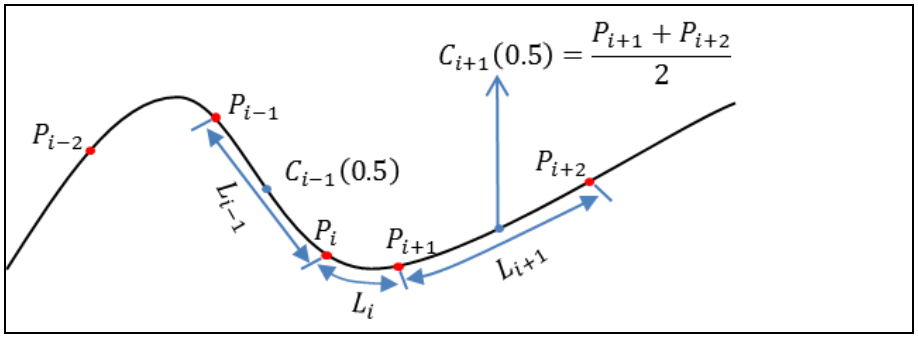

Figure 3. Cubic Spline Interpolation with 5 Points (Case 3)

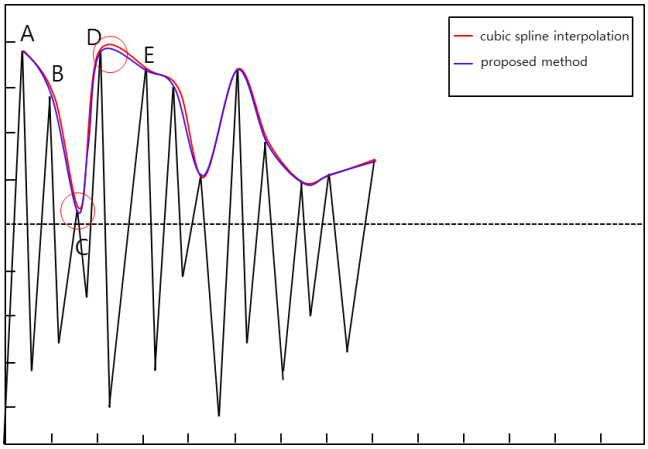

Figure 4. The Result of Improvement Overshooting

Figure 4 shows the compared result using Cubic Spline Interpolation and the suggested method. Following the picture, we can identify that the C and D points improve the overshoot incurred from Cubic Spline Interpolation.

2.2. Neural Network Algorithms

A neural network algorithm [11–13] is a technologically modeled structure of the biological stimulus transmission process by neurons. The objective of a neural network is to develop a high-performance algorithm to process signals that are difficult to process using a conventional sequential algorithm, such as the visual, tactile, and auditory senses used by humans and other living organisms. For this purpose, various neural network algorithms have been proposed. Contrary to conventional sequential algorithms, neural network algorithms have parallel structures in various forms. The most frequently used neural network is a multilayered network that can be separated into many dimensions. A multilayered network is composed of many single-layered neural networks that can only be separated linearly. Figure 5 illustrates the structure of a typical multilayered neural network.

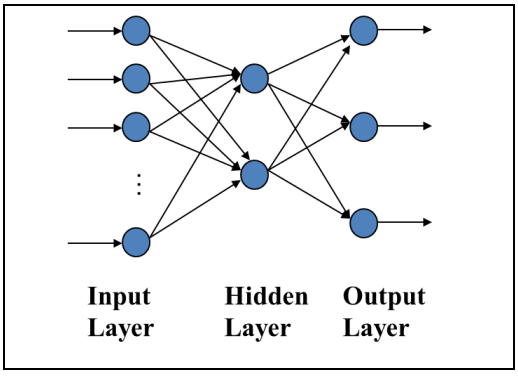

Figure 5. The Structure of Neural Networks

In the recognition process of a neural network, the input signal to the input layer is multiplied by the synapse connected to the hidden layer (weight) and then transmitted to all the hidden layers. The same procedure is repeated once to determine the output value, and the output is sent to the next layer through the activation function in each layer. The activation function should be a monotone increasing function. Typical activation functions include the identity function, unit function, or sigmoid function. The activation function is related to the activation of

actual neurons, which are activated after being stimulated. In an identity function, activation is performed infinitely according to the stimulus. This concept does not correspond to the activation of actual neurons, being far removed from the intended neural network model. In a unit function, the activation is expressed as constant within a certain stimulus, which is also different from the intended neural network model. A sigmoid function, however, shows vigorous activation within a certain stimulus, and the degree of activation by a stimulus decreases as it approaches the maximum activation. This pattern is similar to that of actual neurons, and thus the sigmoid function is the function that is most frequently used in neural network models. Eq. (2.2) shows a bipolar sigmoid function. The denominator is 1 in a unipolar sigmoid function. Figure 6 shows the sigmoid function.

$$A(t) = \frac{1-\exp(-x)}{1+\exp(-x)} \qquad (2.2)$$

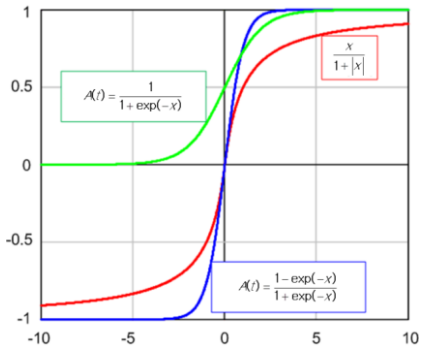

Figure 6. The Sigmoid Function

The most important factor in determining the type of neural network is the learning method to find the weight. In this study, the back-propagation (BP) algorithm, in which the weight is sought by delta learning, was applied. In delta learning, the differential value of the error is used to reduce the error (*i.e.*, the difference between the objective value and the output value). Eq. (2.3) shows the error function of the output value:

$$E_p = \frac{1}{2}\sum_i (t_{pi} - o_{pj})^2 \qquad (2.3)$$

Where tpi denotes the objective output of the unit j in the middle layer in the input vector. The change in weight is given in Eq. (2.4):

$$\Delta_p W_{ij} \propto -\frac{\partial E}{\partial W_{ij}} \qquad (2.4)$$

In the BP algorithm, the weight changes in the backward direction; the output layer weight is first corrected, and then that of the hidden layer is corrected. Figure 7 shows the details of the BP algorithm learning process.

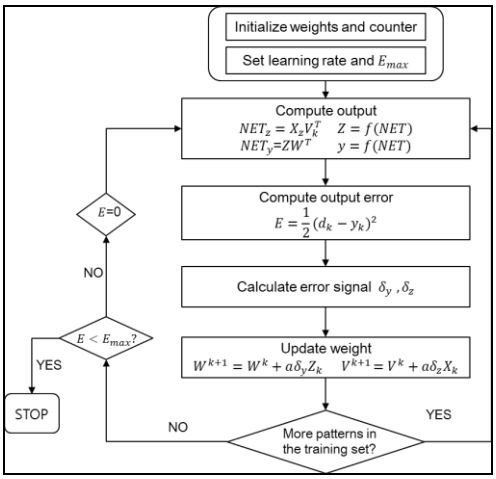

Figure 7. The BP Neural Network Algorithm

3. Experiment and Results

3.1. System Block Diagram

Figure 8 shows a block diagram of the entire system proposed in this article. The signal data collected by the various sensors installed in each component of the wind turbine are gathered by the individual nodes of the WSN and then transmitted to the remote monitoring system through the gateway. The remote monitoring system analyzes the characteristics of the collected signals and diagnoses a fault through the signal analysis algorithm and the neural network. If the result shows a fault, an alarm is given immediately.

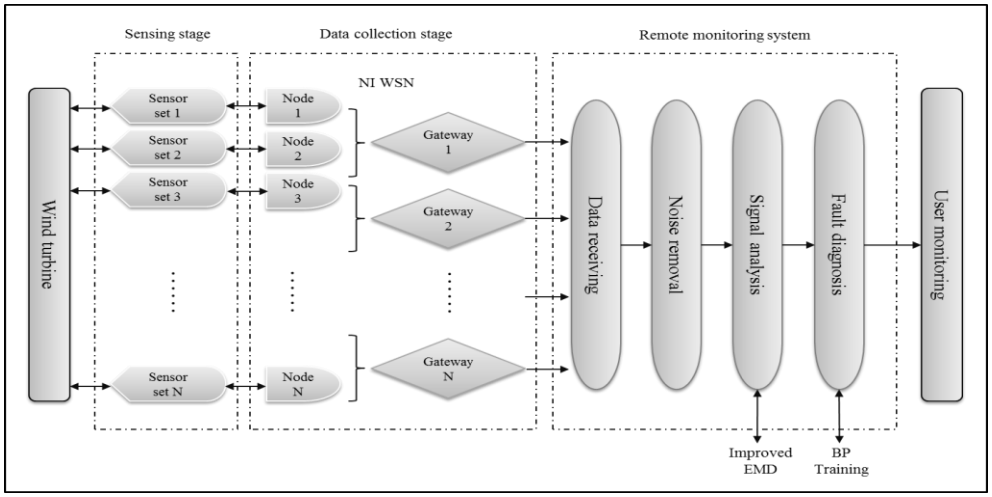

Figure 8. The Block Diagram of the Entire System: Sensing Stage, Constituted with Varies Sensors; Data Collection Stage, which Collects and Transmits the Data by NI WSN; Remote Monitoring System, which Analyzes the Signal and Diagnoses the Faults

3.2. Noise Reduction

The wavelet shrinkage is a typical method for denoising, which is based on wavelet thresholding [13–14]. The theory of this method is that if the calculated wavelet coefficients are not close to the threshold value, they will be assigned 0 to remove the noise. This method has a good effect on the frequency fields higher than

the actual noise level of a signal. If the data of the specific frequency component has a lower value than the noise level, it will be assigned by 0. Additionally, the data that has a lower value will be noise. The method can be divided into three steps.

1. To calculate the wavelet coefficients of the input signal using the wavelet transform until one meets the predetermined level.
2. Perform threshold processing using an appropriate threshold value.
3. Perform the wavelet inverse transform for disposed coefficients to achieve the goal of signal recovery.

Regarding the threshold method proposed by Donoho, there are hard threshold methods and soft threshold methods. Denoise using a soft threshold is simple, convenient, and favored. Therefore, we also used this method for denoising. Figure 10 shows the results of signal denoising using the wavelet transform.

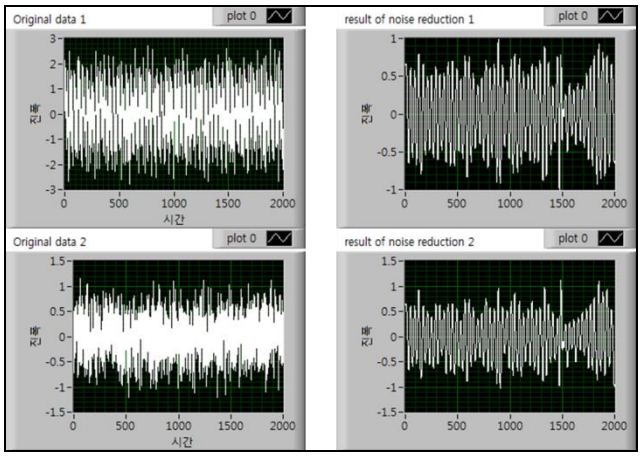

Figure 9. The Results of Noise Reduction by Wavelet Thresholding

3.3. Signal Characteristics Analysis

The primary purpose of wind turbine condition monitoring is to provide an early warning about abnormal conditions. Hence, the signal analysis method basically adopted by most of the condition monitoring system works by setting the alarm generation criteria (signal magnitude) through statistical analysis of the normal signals and testing whether the obtained signal exceeds the criteria.

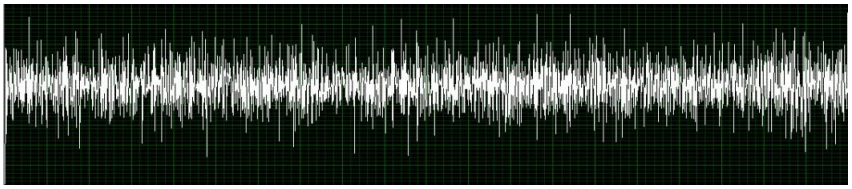

Figure 10. An Example of Normal Signals

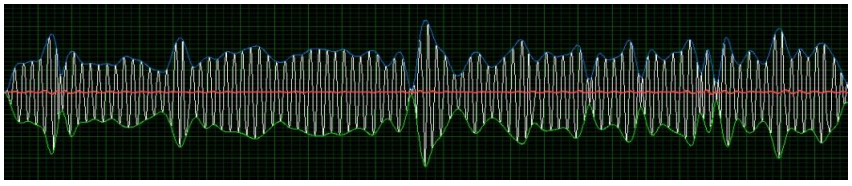

Figure 11. The Enveloping Results by Cubic Spline Removal Overshoot

Figure 11 shows normal vibration signals for the simulation. In this article, EMD was applied to the collected generator vibration signals, assuming that the individual

vibration modes and noises could be independently decomposed from the IMF components obtained by applying EMD to the vibration signals of the generator system. Figure 12 is a spectrum graph showing the envelope as well as the mean values obtained by linking the top and bottom extreme values through cubic spline interpolation in EMD. In Figure 12, the blue line is the envelope connecting the maximum extreme values, while the green line is the envelope connecting the minimum extreme values. The red line connects the mean values.

In the experiment, individual signals were analyzed and compared by EMD through the application of various noises to the normal signals. The frequency elements in normal signals and the signals with which noises were mixed were analyzed to determine whether there was a fault.

3.4. Determination of Generator Faults

Given that vibration signals can change suddenly depending on the wind turbine conditions, the unique characteristics of the normal signals and fault signals are analyzed and classified by neural network learning. In neural network learning, the weight means the parameter between the many inputs and outputs. The weight generally includes a number of local minimum values, and it is sensitive to the initial weight. It is updated by the BP algorithm or by learning. In the BP algorithm, the weight is updated in the backward phase. In the forward phase, the input pattern is presented to the neural network, and the outputs are calculated using the input functions and activation functions for each node. At this point, the input signals are transmitted forward only—that is, toward the output layer. With the weight arbitrarily set at the initial stage, the output value will definitely not agree with the objective value in the output layer, resulting in a large error. In the backward phase, the difference between the objective output and the actual output is calculated to obtain the error, and the weights connecting one layer with another are updated in the direction from the output layer to the input layer. After adjusting the weights, the output calculated with the new input will give a smaller error than that given in the first trial. This process is repeatedly executed until the output aligns with the desired value and the system becomes stable—in other words, when the sum of the errors reaches the predetermined error criteria. More learning data make it easier to find the same pattern and diagnose faults. Although learning takes a longer time in the BP algorithm than in other neural network algorithms, the recognition time is shorter.

In this paper, for analyzing the fault signal (stator imbalance, bearing fault, rotor fault, *etc*.), the neural network training was applied to vibration signal processing. First, according to various classification types, we obtained 30 random samples from 300 frequency components of the fault signal and normal signal separately. Additionally, the natural frequency had been computed for this. Because of the great changes of the generator's vibration frequency, the EMD feature data of eight frequencies for the sampling signal were used for the input layers. Twenty-four hidden layers and four output layers were used.

In this study, neural network learning was performed with respect to generator vibration, unbalanced rotor, and bearing misalignment fault signals. First, regarding individual fault signals and normal signals, the frequency components at 2000 positions were randomly sampled, and their natural frequencies were acquired. For the generator, given that its vibration frequency is greatly affected by wind fluctuation, the three types of fault signals collected at eight positions were used as the output values shown in Table 1, and 24 hidden layers were applied in order to estimate the damage more precisely.

Table 1. The Fault-Type Code

	Output layer			
Type	Stator imbalance	Rotor fault	Bearing fault	Normal
CODE	001	010	100	000

Using a training pattern that estimated the damage frequency and degree of damage, neural network learning was repeated until convergence was achieved. The initial weights of the neural networks were randomly set so that each neural network could conduct learning with different initial weights. In Table 1, the 001 pattern expresses stator imbalance; the 010 pattern expresses rotor faults; the 100 pattern expresses bearing faults; and the 000 pattern expresses normal condition. Table 2 shows examples of the fault detection data with respect to normal signals and fault signal patterns. Table 3 compares the learning results with respect to individual fault signals when the BP algorithm was applied, when the BP + EMD was applied, and when our proposed method was applied. Overall, the learning time in the learning stage was longer when our algorithm was applied than when the BP was applied. However, our algorithm showed a better recognition ratio and a shorter fault recognition time.

Table 2. The Results of Fault Detection

Fault Type	Test value			Input value							
				T0	T1	T2	T3	T4	T5	T6	T7
Stator imbalance	0.0015	0.8901	0.0021	-0.9254	-0.2121	-0.2253	0.7101	0.1335	0.0427	-0.0179	0.0122
Stator imbalance	0.0033	0.9222	0.0027	-0.3257	0.0052	0.0236	0.7225	0.1356	0.0428	-0.0186	0.0127
Stator imbalance	0.0456	0.9013	0.0034	0.0938	0.2821	0.2263	0.7283	0.1370	0.0429	-0.0193	0.0131
Bearing fault	0.8462	0.0352	0.0015	0.3343	0.9239	0.1930	-0.3881	0.0463	0.0324	-0.0343	0.0205
Bearing fault	0.9785	0.0141	0.0062	0.4409	1.0810	0.4969	-0.4568	0.0378	0.0314	-0.0351	0.0213
Bearing fault	0.8802	0.0095	0.0031	-0.5129	0.7145	0.7216	-0.5184	0.0292	0.0303	-0.0360	0.0216
Normal	0.2756	0.0732	0.0385	0.2710	0.1812	0.0546	0.2243	0.0992	0.0384	-0.0293	0.0186
Normal	0.0947	0.2380	0.0104	0.0685	0.1749	-0.0810	0.5984	0.1256	0.0413	-0.0245	0.0161
Rotor fault	0.0001	0.0027	0.7915	-0.3581	-0.1115	-0.1658	-0.7091	-0.0314	0.6246	0.7402	0.0234
Rotor fault	0.0007	0.0814	0.8309	-0.4109	-0.1298	-0.0743	0.6305	-0.0345	0.7344	0.0635	0.6456
Rotor fault	0.0031	0.0175	0.9651	0.0405	-0.6551	0.0124	0.8009	0.4640	0.0413	1.0805	0.2806

4. Conclusion

To address the location limitations of wind turbines that may have various faults due to environmental factors, this article proposes a communication network that transmits vibration signals collected by various sensors to a remote monitoring system through the establishment of the NI WSN system. Signal analysis using HHT was proposed as an efficient fault diagnosis method. HHT presents the frequency domain components under phase shift on the polar coordinates, as well as amplitude information on individual signals. Hence, HHT can present information in the time-frequency domain in a manner similar to that of STFT and the wavelet transform. In addition, HHT decomposes signals into signals with different internal frequency

components, beginning with high-frequency components. The frequency components decomposed in this way have independent characteristics, whose detection can be used to accurately diagnose faults in offshore wind turbines through BP neural network learning. To test the efficiency of the proposed algorithm, learning was performed with three fault signals: Generator vibration, an unbalanced rotor, and bearing misalignment. The results showed that the BP algorithm was more efficient in terms of recognition ratio and recognition time than the general neural network learning algorithms. The proposed method may be applied to the analysis of mechanical and electrical faults in various industries.

Acknowledgment

This work was supported by the Human Resources Development program (No. 20134030200320) of the Korea Institute of Energy Technology Evaluation and Planning (KETEP) grant funded by the Korea government Ministry of Trade, Industry and Energy.

References

[1] E. C. Lee and S. J. Mo, "Outlook and Competitive Analysis of the Domestic Wind Power Industry", Hana Institute of Finance, no. 17, **(2009)**.
[2] C. O. Shin and G. H. Yuk, "Environmental and Economic Impacts of Offshore Wind Power", Korea Maritime Institute, **(2011)**.
[3] R. W. Hyers, J. G. McGowan, K. L. Sullivan, J. F. Manwell and B. C. Syrett, "Condition monitoring and prognosis of utility scale wind turbine", Energy Material, vol. 1, no. 3, **(2011)**, pp. 187-203.
[4] P. Caselitz and J. Giebhardt, "Rotor condition monitoring for improved operational safety of offshore wind energy converters", Journal of Solar Energy Engineering, vol. 127, **(2005)**.
[5] M. S. An and D. S. Kang, "Implementation of Remote Condition Monitoring System of Offshore Wind Turbine Based on NI WSN", SERSC International Journal of Control and Automation, vol. 6, no. 2, **(2013)**, pp. 325-334.
[6] A. Bellini, A. Yazidi, F. Filippetti, C. Rossi and G. A. Capolino, "High frequency resolution techniques for rotor fault detection of induction machines", IEEE Transactions on Industrial Electronics, vol. 55, no. 12, **(2008)**, pp. 4200-4208.
[7] M. Wilkinson, F. Spinato and P. Tavner, "Condition monitoring of generators and other subassemblies in wind turbine drive trains", IEEE Diagnostics for Electrical Machines, Power Electronics and Drives, Cracow, Poland, **(2007)**, pp. 388-392.
[8] N. E. Huang, Z. Shen, S. R. Long, M. L. Wu, H. H. Shih, Q. Zheng, N. C. Yen, C. C. Tung and H. H. Liu, "The empirical mode decomposition and Hilbert spectrum for nonlinear and non-stationary time series analysis", Proceeding Roy. Soc. London A, vol. 454, no. 1971, **(1998)**, pp. 903–995.
[9] D. S. Gu, "Comparison of Hilbert and Hilbert-Huang Transform for The Early Fault Detection by using Acoustic Emission Signal", Journal of the Korean Society of Marine Engineering, vol. 36, no. 2, **(2012)**, pp. 258-266.
[10] Y. J. Li and P. W. Tse, "EMD-based fault diagnosis for abnormal clearance between contacting components in a diesel engine", Mechanical Systems and Signal Processing, vol. 23, no. 1, **(2010)**, pp. 193-210.
[11] K. M. Silva, B. A. Souza and N. S. D. Brito, "Fault detection and classification in transmission lines based on wavelet transform and ANN", IEEE Transactions on Power Delivery, vol. 21, no. 4, **(2006)**, pp. 2058-2063.
[12] C. S. Oh, "Neuro Computer", NEAHA Publisher, Seoul, **(2000)**.
[13] H. N. Robert, "Theory of the back propagation neural network", Neural Networks, 1989. IJCNN, International Joint Conference on IEEE, Washington, DC, USA, **(1989)**.
[14] M. Arai, K. Okumura, M. Satake and T. Shimizu, "Proteome-wide functional classification and identification of prokaryotic trans-membrane proteins by trans-membrane topology similarity comparison", Protein Science, vol. 13, no. 8, **(2004)**, pp. 2170-2183.

Authors

Ming-Shou An, He received a B.S. degree from YANBIAN University, China, in 2007, an M.S. degree from Dong-A University, in 2009.He now is a PhD candidate of the Department of Electronic Engineering, Dona-A University, Busan, Korea. His research interests are signal processing and pattern recognition.

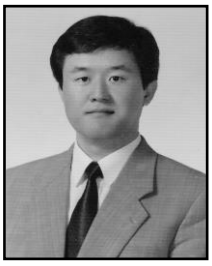

Dae-Seong Kang, He received a B.S. degree from Kyungpook National University, Daegu, Korea, in 1984, M.S. degree and D.Sc. degree in electrical engineering from Texas A&M University, in 1991 and 1994, respectively. He is currently full professor of the Department of Electronic Engineering, Dona-A University, Busan, Korea. His research interests are image processing and compression.